ACS APPLIED MATERIALS & INTERFACES

Article

A Self-Powered Wearable Non-invasive Electronic-Skin for Perspiration Analysis Basing on Piezo-Biosensing Unit Matrix of Enzyme/ZnO Nanoarrays

Wuxiao Han, Haoxuan He, Linlin Zhang, Chuanyi Dong,
Hui Zeng, Yitong Dai, Li-Li Xing, Yan Zhang, and Xinyu Xue

ACS Appl. Mater. Interfaces, **Just Accepted Manuscript** • DOI: 10.1021/acsami.7b07990 • Publication Date (Web): 07 Aug 2017

Just Accepted

ACS Publications

ACS Applied Materials & Interfaces is published by the American Chemical Society.
1155 Sixteenth Street N.W., Washington, DC 20036

A Self-Powered Wearable Non-invasive Electronic-Skin for Perspiration Analysis Basing on Piezo-Biosensing Unit Matrix of Enzyme/ZnO Nanoarrays

Wuxiao Han,[†] Haoxuan He,[†] Linlin Zhang,[†] Chuanyi Dong,[†] Hui Zeng, [†] Yitong Dai, [†] Lili Xing,[†] Yan Zhang,*[‡] and Xinyu Xue*[†]*

[†]College of Sciences, Northeastern University, Shenyang 110004, China

[‡]School of Physical Electronics, University of Electronic Science and Technology of China, Chengdu 610054, China

*Corresponding Author

KEYWORDS: self-powered, electronic-skin, piezoelectric effect, enzymatic reaction, perspiration analysis.

ABSTRACT

The emerging multifunctional flexible electronic-skin for establishing body-electric interaction can enable real-time monitoring of personal health status as a new personalized medicine technique. A key difficulty in the device design is the flexible power supply. Here, a self-powered wearable non-invasive electronic-skin for perspiration analysis has been realized basing on piezo-biosensing unit matrix of enzyme/ZnO nanoarrays. The electronic-skin can detect lactate, glucose, uric acid and urea in the perspiration, and no outside electricity power supply or battery is used in the biosensing process. The piezoelectric impulse of the piezo-biosensing units

serves as the power supply and biosensing data. The working mechanism can be ascribed to the piezoelectric-enzymatic-reaction coupling effect of enzyme/ZnO nanowires. The electronic-skin can real-time/continuously monitor the physiological state of a runner through analyzing the perspiration on his skin. This approach can promote the development of new-type body electric and self-powered biosensing electronic-skin.

1. INTRODUCTION

The emerging multifunctional flexible sensor (e.g. electronic-skin) for establishing body-electric interaction is one of the most important subjects that many researchers are focusing on.[1-5] A variety of new multifunctional flexible electronic-skins (skin-implanted, organic-patched or skin-surface devices) accompanying with body activities have been studied for future medical care, such as detecting blood glucose, blood pressure, arterial stiffening, heart rate, electrolyte balance, body temperature, breathing rate and etc..[6-14] These wearable electronic-skins and other flexible biosensors can achieve real-time detection of personal physiological metabolic indicators, and they can realize continuous detection of personal health status as a new personalized medicine technique.[15-19] And diverse wearable non-invasive perspiration-analysis biosensors have been developed for accurate measurement of the physiological state, which can avoid the inconvenience for the traditional invasive blood sampling approach.[20-24] Nowadays, an attractive research has been reported that a fully integrated multiplexed biosensor array system can extract the complex available information from different biomarkers in the perspiration secretion.[25]

For the further development of wearable non-invasive perspiration-analysis biosensors, the next generation of device requires the following distinct features. The device needs to be

designed as mechanically flexible and has conformable integration with body through working on the skin surface or alongside the organic/tissue (not like pocket medical electronics).[26-27] The device also needs to include multi-functional biosensor arrays, which can simultaneously and selectively measure different analytes (such as glucose, lactate, sodium ions, potassium ions, skin temperature and etc.).[28] The third key difficulty in the device design is the flexible power supply for driving individual biosensors. The traditional bulky battery is not suitable for the wearable skin-like device and the distribution of power units needs to be solved.[29-32]

In human perspiration, biological molecules and inorganic salts contain a wealth of physiological information, and non-invasive monitoring on the human body can be achieved through the analysis of perspiration composition.[33-34] Taking lactate as an example, lactate is the important metabolite of the anaerobic glycolytic pathway and the concentration of lactate in perspiration can be proposed to evaluate the fitness level.[35] Lactate monitoring is significant in sport medicine, which can assess the maximum performance of athletes in high-intensity activities.[36] Lactate in perspiration can also act as an useful marker of tissue vitality and may provide advance warning for pressure.[37] So, the lactate concentration is directly interrelated to the physiological condition.[38] For other biomarkers, glucose is reported to be metabolically associated with blood glucose;[39] perspiration uric acid is the major metabolite of purine in human body and it serves as a key marker biomolecule for the detection of diseases related to gout, purine metabolism, leukemia and the change of urate level in other body fluids (blood, urine and etc.);[40-41] the detection of urea concentration in the perspiration is also a significant method for some disease diagnosis.[42] Generally, the compositions of perspiration and blood are osmotically related. Thereby, perspiration can be used to analyze physiological status and personal diseases without taking an invasive blood sampling.[43]

In this paper, a self-powered wearable non-invasive electronic-skin for perspiration analysis basing on piezo-biosensing unit matrix of enzyme/ZnO nanoarrays has been presented. The enzymes modified on the surface of ZnO nanowires include LOx (lactate oxidase), GOx (glucose oxidase), uricase and urease. The electronic-skin can detect lactate, glucose, uric acid and urea in the perspiration through actively outputting piezoelectric signal (driven by body movement). The piezoelectric output of the piezo-biosensing unit is dependent on the analyte concentration in the perspiration, which can be treated as the power supply and the biosensing data. In this piezo-biosensing process, no outside electricity power supply or battery is used. The working mechanism is ascribed to the piezoelectric-enzymatic-reaction coupling process of enzyme/ZnO nanowires. The electronic-skin can be attached on the forehead of a runner, and real-time/continuously monitor his physiological state. This research approach may probably point out the developing orientation of novel self-powered multifunctional electronic-skin.

2. EXPERIMENTAL SECTION

2.1. Synthesis of ZnO Nanowire Arrays. The chemical reagents for the preparation of ZnO nanowire arrays were provided by Sinopharm Chemical Reagent Co. Ltd. A seed-assisted hydrothermal method was used to synthesize vertically-aligned ZnO nanowire arrays on Ti substrate.[44-48]

2.2. Fabrication of Self-Powered Wearable Non-Invasive Electronic-Skin. The pre-cleaned Kapton substrate was used to support the device. Horizontally-aligned ZnO nanowire arrays (overwhelmed down) were the core materials in the device. The fabrication process (depositing interdigital electrode pattern), including photolithography and electron-beam evaporation processes, is similar to the previous report.[45,49] A ZnO nanowire (length: ~12 μm) could cross the

electrode couple (distance: 5 μm). The distance between neighboring electrode couples was 20 μm, ensuring the same c-axis direction of all ZnO nanowires.

2.3. Modifying Enzyme on the Surface of ZnO Nanowires. ZnO nanowires of four different piezo-biosensing units in the electronic-skin were then modified with LOx, GOx, uricase and urease, respectively. LOx, GOx, uricase and urease were supplied by Sigma Chemical Co. St. Louis, MO, USA. LOx solution (2 μL, 10 mg mL^{-1} in PBS) was slowly dropped onto the lactate-biosensing unit, and an incubation procedure was conducted in fume hood for two hours. After repeating this process for four times, the substrate was rinsed by deionized water for removing the unadsorbed LOx. The modification processes of GOx (2 μL, 10 mg mL^{-1} in PBS), uricase (2 μL, 5 mg mL^{-1} in PBS) and urease (2 μL, 15 mg mL^{-1} in PBS) were performed on the glucose, uric acid and urea -biosening units in the same way, respectively. The electronic-skin was dried naturally in dark. The enzyme solutions were stored at 4°C.

2.4. Measurement. The electronic-skin was stuck on a polystyrene board (fixed in a petri dish in a sealed dark box) and immersed in test solutions (pure water, lactate aqueous solution, glucose aqueous solution, uric acid aqueous solution and urea aqueous solution). Sodium lactate reagent, glucose, urea and uric acid were supplied by Sigma Chemical Co. St. Louis, MO, USA. For generating bending deformation on the electronic-skin, a hammer (linked to a motor) was used to provide the force. The magnitude of the force was measured by a force detector. A low-noise preamplifier (Model SR560, Stanford Research Systems) was used to measure the piezoelectric output of the device. The lactate, glucose, uric acid and urea concentrations of the test solutions were close to those in human perspiration.

3. RESULTS AND DISCUSSION

The experimental design, device architecture and fabrication procedure of the self-powered wearable non-invasive electronic-skin are exhibited in Figure 1. Figure 1a shows that the electronic-skin can be attached on the surface of a runner at different body parts and monitor the physiological status by analyzing perspiration components. Figure 1b is the optical picture of the electronic-skin in our test (1.4×1.5 cm). Four piezo-biosensing units are aligned in the test device, and the Kapton substrate is used to provide bending deformation space.[50] Figure 1c shows that the electronic-skin can be easily attached on human wrist for self-powered perspiration analysis. Fingers can provide pressing force on the device, and each piezo-biosensing unit can generate piezoelectric signal.[51] The four electrode couples are connected to the outside circuit with eight copper leads (fixed with silver glue). In this experiment, the four piezo-biosensing units are tested separately.

As the electronic-skin can work in liquid solution, it can directly and real-time collect data from the perspiration, as schematically shown in Figure 1d. The four piezo-biosensing units modified with LOx, GOx, uricase and urease in the electronic-skin can detect lactate, glucose, uric acid and urea, respectively. Upon applied deformation, the piezoelectric impulse of the piezo-biosensing units (immersed in the perspiration) can be recorded through Ti electrodes. The piezoelectric output is dependent on the enzymatic reaction between the enzyme and corresponding perspiration component, acting as not only the biosensing signal but also the electricity power for driving the device. The measurement setup is shown on the right bottom corner of Figure 1d. In the whole perspiration analysis process, the electronic-skin does not need external electricity power supply or battery, showing a good potential for long-term working with human body through harvesting the mechanical energy of body motion.

The whole pattern of the electronic-skin is shown in Figure 1e. 6×6 piezo-biosensing units are aligned on the device, which can be extended to detect up to 36 biomarkers in the perspiration. In this test, a small part of 2×2 piezo-biosensing units is used. The fabrication process of the electronic-skin is schematically shown in Figure 1f. The detailed fabrication process of the electronic-skin is described in experimental section.

The characterization of the material and device is exhibited in Figure 2. X-ray diffraction (XRD, D/max 2550 V, CuKα Radiation) is used to confirm the crystal phase of ZnO. Figure 2a shows the XRD pattern of ZnO nanowires, and the diffraction peaks can be indexed to ZnO (JCPDS file NO. 36-1451). Transmission electron microscope (TEM, JEOL JEM-2010) and scanning electron microscope (SEM, JEOL JSM-6700F) are used to investigate the microstructure of ZnO and the device. Figure 2b is TEM image of ZnO nanowires, showing that the nanowire with the growth direction of c-axis is monocrystalline. The planar distance of the (002) plane is 0.52 nm (wurtzite structure of ZnO).[52-53] The top view of ZnO nanowire arrays is shown in Figure 2c. The vertically-aligned nanowires with the same growth direction have the diameters of ~300 nm. Figure 2d shows the side view of ZnO nanowire arrays. The nanowires have the lengths of ~12 μm. Figure 2e is the enlarged view of the heads of ZnO nanowires, showing the hexagon-shaped cross section. Figure 2f shows the horizontally-aligned ZnO nanowires after being overwhelmed down in the same direction on Ti substrate. Figure 2g shows ZnO nanowires smearing on Kapton substrate. ZnO nanowires are in the similar direction with random angular deviation. Figure 2h shows the partial region of the device before removing photoresists. Figure 2i shows single ZnO nanowire bridging the Ti electrodes after removing photoresists.

The electronic-skin connecting to the outside circuit is immersed in lactate, glucose, uric acid and urea aqueous solutions for measuring the piezo-biosensing performance, respectively. Figure 3 shows the piezo-lactate-sensing behavior of the piezo-biosensing unit modified with LOx. Under applied compressive force of 20 N, the piezo-biosensing unit can actively output piezoelectric voltage (piezoelectric properties of LOx/ZnO nanowires), and the piezoelectric impulse is obviously dependent on the lactate concentration in the aqueous solution (Figure 3a). The outputting piezoelectric voltage stabilizes at 23.5 mV in pure water. After the lactate concentration changing to 2.00 mM L^{-1}, the outputting piezoelectric voltage decreases to 18.2 mV. As the lactate concentration increases, the outputting piezoelectric voltage decreases. As the lactate concentration is 0.00, 2.00, 5.00, 8.57, 13.44 and 20.00 mM L^{-1}, the outputting piezoelectric voltage of the piezo-biosensing unit is 23.4, 18.2, 13.8, 11, 6.2 and 3 mV (Figure 3b), respectively. These results suggest that the piezo-biosensing unit (with LOx modification) in the electronic-skin can rapidly detect the lactate concentration and simultaneously output the biosensing signal. Figure 3c-e shows the detail of the piezoelectric impulse. The response of the piezo-biosensing unit can be simply defined as:[54]

$$R\% = \left|\frac{V_0 - V_i}{V_i}\right| \times 100\% \quad (1)$$

, where V_0 and V_i are the outputting piezoelectric voltage of the piezo-biosensing unit in pure water and lactate aqueous solution, respectively. The response of the piezo-biosensing unit is in function of the lactate concentration, as shown in Figure 3b. The response against 2.00, 5.00, 8.57, 13.44 and 20.00 mM L^{-1} lactate is about 28.6, 69.6, 112.7, 278.0 and 680.0, respectively. Figure 3f shows that the detection limit of lactate piezo-biosensing unit is about 0.10 mM L^{-1} and the resolution is about 0.10 ± 0.05 mM L^{-1}.

As a control experiment, the piezo-biosensing unit modified with LOx is immersed in different volumes of pure water. In Figure 3g, the piezoelectric output of the piezo-biosensing unit almost keeps constant as pure water is added in the test petri dish. The outputting piezoelectric voltage and the response in different volumes of pure water are shown in Figure 3h. As the water volume is 25, 30, 35, 40 and 45 mL, the outputting piezoelectric voltage of the electronic-skin is 26.1, 26.3, 26.6, 27.3 and 27.1 mV, respectively. And none response is obtained. As another control experiment, a piezo-biosensing unit without LOx modification is immersed in different concentration of lactate aqueous solution. Figure 3i shows the outputting piezoelectric voltage of the piezo-biosensing unit (without LOx modification) in lactate aqueous solutions. As the lactate concentration increases, the outputting piezoelectric voltage keeps constant. As shown in Figure 3j, as the lactate concentration is 0, 2, 5, 8.57, 13.44 and 20 mM L^{-1}, the outputting piezoelectric voltage of the piezo-biosensing unit (without LOx modification) is 29.3, 32.1, 30.7, 30.2, 33.8 and 26.9 mV, respectively. And none response is obtained. These control experiments demonstrate that the lactate-sensing behavior of the piezo-biosensing unit with LOx modification arises from the enzymatic reaction between LOx and lactate.

Figure 4a exhibits the piezo-lactate-sensing performance of the piezo-biosensing unit (with LOx modification) in the electronic-skin under different forces (20, 32 and 40 N). The applied forces have the same frequency (1.0 Hz). Under the force of 20 N, the outputting piezoelectric voltage of the piezo-biosensing unit against 0, 1, 3.33, 6.42, 11.63 and 15.56 mM L^{-1} lactate is 19.1, 15, 11.5, 6.5, 3.7 and 3.4 mV, respectively. Under the force of 32 N, the outputting piezoelectric voltage is 79, 66, 51.3, 37.3, 28.5 and 14.4 mV, respectively. Under the force of 40 N, the outputting piezoelectric voltage is 222.6, 201.9, 110.8, 74.8, 51.5 and 44 mV, respectively. As the applied force increases, the outputting piezoelectric voltage increases.

Coincidentally, the responses of the piezo-biosensing unit under different applied forces are almost similar, as shown in Figure 4b and c. This result demonstrates that the electronic-skin has loose operation condition and can be easily used in practical physiological state monitoring.

Flexibility or stretchability is a key factor of the electronic-skin in practical application because the device attached on human skin needs to accompany with body activities all the day.[55] The piezo-lactate-sensing performance of the piezo-biosensing unit (with LOx modification) in the electronic-skin against 15.56 mM L^{-1} lactate with different bending angles is shown in Figure 4d. In this study, the bending angle changes with the moving distance of the motor (force: 40 N). As the bending angle is 18°, 12° and 8°, the outputting piezoelectric voltage of the device in 0 mM L^{-1} lactate solution is 222.6, 79 and 19.1 mV. And the voltage in 15.56 mM L^{-1} lactate solution is 44, 14.4 and 3.4 mV, respectively. The relationship between the bending angle and outputting piezoelectric voltage (as well as the response) is shown in Figure 4e. Coincidentally, the responses of the piezo-biosensing unit under different bending angles are almost the same. This feature can further facilitate the practical operation of the electronic-skin.

The wearable biosensors need to adapt the repeated stress of body motion and physical exercise.[56] Figure 4f shows the stability of the piezo-biosensing unit (with LOx modification) in the electronic-skin during bending for many times. The testing lactate concentration is 11.63 mM L^{-1}; the applied force is 40 N; and the bending angle is 18°. After bending for 100, 200, 300, 400, 500, 600, 700 and 800 times, the response is 138, 130, 132, 134, 142, 135, 144 and 140, respectively. High stability of the electronic-skin has been achieved, being beneficial for practical applications. The device is effective in 3~6 days due to the enzyme activity, and regularly replenishing enzymes can solve this problem. Titanium as the electrode can avoid a

certain degree of corrosion, but ZnO may have the corrosion problem. To prolong the lifetime of the device, new material system needs to be further developed.

The piezo-biosensing units modified with different enzymes (GOx, uricase and urease) in the electronic-skin can detect glucose, uric acid and urea concentration in the perspiration, respectively. The experimental results are exhibited in Figure 5. Under different applied compressive forces, the piezo-biosensing units can generate piezoelectric impulse, and the piezoelectric output is obviously dependent on the corresponding biomarker concentration in the aqueous solutions. Figure 5a shows the piezo-glucose-sensing performance of the piezo-biosensing unit (with GOx modification) under the applied force of 32 N. The initial piezoelectric voltage stabilizes at 64.6 mV in pure water. As the glucose concentration increases to 0.042, 0.083, 0.125, 0.166 and 0.208 mM L^{-1}, the outputting piezoelectric voltage decreases to 56.4, 51, 44.8, 35.8 and 29 mV, respectively. As the glucose concentration increases, the outputting piezoelectric voltage decreases. Figure 5b shows the piezo-glucose-sensing performance of the piezo-biosensing unit (with GOx modification) in the electronic-skin under different forces (20, 32 and 40 N). Figure 5c and d show the responses of the piezo-biosensing unit under different applied forces and glucose concentration. Figure 5e shows the piezo-uric-acid-sensing performance of the piezo-biosensing unit (with uricase modification) under the force of 32 N. The initial piezoelectric voltage stabilizes at 60 mV in pure water. As the uric acid concentration increases to 0.024, 0.044, 0.063, 0.082 and 0.101 mM L^{-1}, the voltage decreases to 50, 38, 31, 22.4 and 14.6 mV successively. Figure 5f shows the piezo-uric-acid-sensing performance of the piezo-biosensing unit in the electronic-skin under different forces (20, 32 and 40 N). Figure 5g and h show the responses of the piezo-biosensing unit (with uricase modification) under different applied forces and uric acid concentration. Figure 5i shows the

piezo-urea-sensing performance of the piezo-biosensing unit (with urease modification) under the force of 32 N. The initial piezoelectric voltage stabilizes at 67 mV in pure water. As the urea concentration increases to 5, 10, 15, 20 and 25 mM L^{-1}, the voltage decreases to 61, 37.6, 32.2, 22.6 and 15.6 mV, respectively. Figure 5j shows the piezo-urea-sensing performance of the piezo-biosensing unit in the electronic-skin under different forces (20, 32 and 40 N). Figure 5k and l show the responses of the piezo-biosensing unit (with urease modification) under different applied forces and urea concentration. Figure 5m exhibits the piezo-glucose-sensing unit has the detection limit of ~0.02 mM L^{-1}, and the resolution of the biosensor is 0.02 ± 0.005 mM L^{-1}. Figure 5n exhibits the detection limit of the piezo-uric-acid-sensing unit is ~0.01 mM L^{-1}, and the resolution of the biosensor is 0.01 ± 0.005 mM L^{-1}. Figure 5o exhibits the piezo-urea-sensing unit has the detection limit of ~0.5 mM L^{-1}, and the resolution of the biosensor is 0.5 ± 0.2 mM L^{-1}.These results suggest that the piezo-biosensing units with different enzyme modification in the electronic-skin can rapidly detect glucose, uric acid and urea concentrations in the perspiration.

For biosensors, the selectivity is a significant parameter in practical application for distinguishing various biomarkers. The selectivity of the four piezo-biosensing units (modified with LOx, GOx, uricase and urease) in the electronic-skin against lactate, glucose, uric acid and urea in the perspiration is shown in Figure 6. As shown in Figure 6a, the piezo-biosensing unit modified with LOx can only detect lactate, and the responses against glucose, uric acid and urea are nearly zero. As shown in Figure 6b-d, the piezo-biosensing units modified with GOx, uricase and urease can only detect glucose, uric acid and urea, respectively. High selectivity of the piezo-biosensing units in the electronic-skin has been obtained, which is very significant for practical applications of the electronic-skin.

The piezo-biosensing performance arises from the coupling effect between the surface enzymatic reaction (LOx and lactate, GOx and glucose, uricase and uric acid, urease and urea) and the piezoelectric characteristic of ZnO nanowire. The piezoelectric property of ZnO nanowires and their application as piezo-nanogenerator have been widely investigated.[6, 13, 53] When the deformation applied to the c-axis of ZnO nanowire, intrinsic polarization appears inside the nanowire, resulting in the presence of positive and negative charges on the opposite surfaces of the nanowire.[57] The piezoelectric negative/positive charges can create the piezoelectric potential, which can lead to the piezoelectric output in the external circuit through driving electrons in the load migrating between the two electrodes.[58] Simultaneously, the piezoelectric field can also drive the carriers inside ZnO nanowire migrating. In this process, the carrier migration partially screens the piezoelectric field, which reduces the piezoelectric output of the nanowire.[59] The piezo-screening effect of ZnO nanowire can be affected by the carrier density inside the nanowire.[60] Our previous reports have described that the surface adsorption of bio/chemical molecules can change the surface carrier density of ZnO nanowire, thereby changing the piezo-screening effect and influencing the piezoelectric impulse.[61-63] In this work, the enzymatic reactions (LOx and lactate, GOx and glucose, uricase and uric acid, urease and urea) can enhance the surface carrier density of ZnO nanowire, thus strengthening the piezo-screening effect and decreasing the piezoelectric impulse.

Figure 7 schematically illustrates the detailed working mechanism of the piezo-biosensing units in the electronic-skin. As shown in Figure 7a, the four piezo-biosensing units in the electronic-skin are modified with the LOx, GOx, uricase and urease, respectively. The enzyme/ZnO nanowires are crossing on the interdigital electrodes (Figure 7b). Under applied force, the enzyme/ZnO nanowires can be bended, as shown in Figure 7c. In pure water (Figure

7d and e), LOx@ZnO nanowire has not come into contact with lactate. The nanowire without applied deformation has zero piezoelectric voltage (Figure 7d). The nanowire can output piezoelectric impulse with applied deformation (Figure 7e). As the enzymatic reaction does not take place, the surface carrier density is low, and the weak piezo-screening effect results in high outputting piezoelectric voltage. As shown in Figure 7f and g, after the nanowire being immersed in lactate aqueous solution, the enzyme reaction between LOx and lactate takes place. At the first step, pyruvate and H_2O_2 are produced as follows:[64]

$$Lactate + H_2O + O_2 \xrightarrow{LOx} pyruvate + H_2O_2 \quad (2)$$

It has been reported that H_2O_2 can transfer electrons into ZnO nanowire and increase the surface carrier density through producing H^+ and e^- by the following decomposition process:[65]

$$H_2O_2 \rightarrow 2H^+ + O_2 + 2e^- \quad (3)$$

In this process, H^+ ion (as extra carriers) adsorption can also take place on the nanowire.[66] Under applied deformation (Figure 7g), the outputting piezoelectric voltage of ZnO nanowire is reduced due to the strong piezo-screening effect from the large amount of H^+ and e^- on the surface of the nanowire. The other three enzymatic reactions are shown in Figure 7h. The enzymatic reaction between GOx and glucose can produce gluconic acid and H_2O_2,[67] and then H_2O_2 can increase the surface carrier density through producing H^+ and e^-. The enzymatic reaction between uricase and uric acid can produce allantoin and H_2O_2,[68] and then transmitting extra carriers into ZnO nanowires. The enzymatic reaction between urease and urea can produce NH_4^+ and H^+.[69] In this process, NH_4^+ and H^+ ions as extra carriers can be absorbed on the nanowire.

A practical application of the wearable non-invasive electronic-skin on the skin of a runner for perspiration analysis (detecting lactate, glucose, uric acid and urea) without outside electricity power source is shown in Figure 8. As shown in Figure 8a, the four piezo-biosensing units are modified with LOx, GOx, uricase and urease, respectively. The electronic-skin is attached on the forehead of a runner, as shown in Figure 8b. Figure 8c shows the tester running with different speed. Firstly, the tester runs for 8 min (speed: 6 km h^{-1}). And the electronic skin is pressed under a continuous and stable force by finger, and the piezoelectric is detected using a low-noise preamplifier. The outputting piezoelectric voltage of the four piezo-biosensing units (with LOx, GOx, uricase and urease modification) is 72.4, 57.8, 72.8 and 57.6 mV, respectively (Figure 8d). Then the person keeps running for 30 min (speed: 12 km h^{-1}). And the subject of the running test does not have water intake in all the process. The electronic-skin is pressed under a continuous and stable force by finger (the magnitude of the force are the same as before). The outputting piezoelectric voltage of the four piezo-biosensing units (with LOx, GOx, uricase and urease modification) is 28.2, 39.2, 40.4 and 45 mv, respectively (Figure 8e). The two sweat samples are collected from the forehead of the tester, and the specific concentrations of these four biomarkers are ex-body tested using standard analyzer. For the sweat sample of the tester who runs for 8 min (speed: 6 km h^{-1}), the concentration of lactate, uric acid and urea is about 4.958, 0.041 and 4.50 mM L^{-1}, respectively. For the sweat of the tester who runs for 30 min (speed: 12 km h^{-1}), the concentration of lactate, uric acid and urea is about 13.044, 0.148 and 9.50 mM L^{-1}, respectively. The glucose concentration is too small to test, and the previous literature confirms that the glucose concentration may increase with vigorous exercise for ~20 min.[25] Figure 8f shows the comparison of the response (piezo-biosensing) between on-body and ex-body testing. For lactate analyzing, the data are similar. These results show that the concentration of the four biomarkers

in the perspiration increases with time (30 min), especially the lactate concentration. This is coincident with the fact that lactate is constantly produced during normal metabolism and physical exercise.[70] Due to the accumulation of body metabolism, the body sweat can release some biomarkers (including glucose, uric acid and urea) in the sports. With the increase in exercise intensity and duration, the sweat with these biomarkers is constantly being discharged on the skin, the result is similar to other research findings.[25, 39, 71-73] Continuous monitoring of the human subject's physiological status by analyzing the perspiration has been realized using the self-powered wearable non-invasive electronic-skin. The electronic-skin can detect lactate, glucose, uric acid and urea concentrations in human perspiration, demonstrating potential applications for sports medicine and related clinical monitoring. In future work, we will further try to bridge the current technology between power supplying, electrical signal conversion, signal modulation and signal processing in the wearable and fully integrated electronic-skins.

4. CONCLUSIONS

In conclusion, a self-powered wearable non-invasive electronic-skin for perspiration analysis has been realized basing on piezo-biosensing unit matrix of enzyme/ZnO nanoarrays. The piezo-biosensing units in the electronic-skin can detect lactate, glucose, uric acid and urea in the perspiration through actively outputting piezoelectric signal, and the outputting piezoelectric signal can be treated as power supply and the biosensing data. All the biosensing process does not use any outside electricity power supply or battery. The new piezoelectric-enzymatic-reaction coupling effect has been proposed. The device attached on the human skin can real-time/continuously monitor the physiological state during running. The present results can promote the investigation of body electric and self-powered biosensing electronic-skin.

AUTHOR INFORMATION

Corresponding Author

* E-mail addresses: xuexinyu@mail.neu.edu.cn (X. Xue); xinglili@mail.neu.edu.cn (L. Xing); zhangyan@uestc.edu.cn (Y. Zhang).

Notes

The authors declare no competing financial interest.

ACKNOWLEDGEMENTS

This work was supported by the National Natural Science Foundation of China (11674048), the Fundamental Research Funds for the Central Universities (N150505001 and N160502002), Liaoning Natural Science Foundation (2015021009), and Liaoning BaiQianWan Talents Program (2014921017).

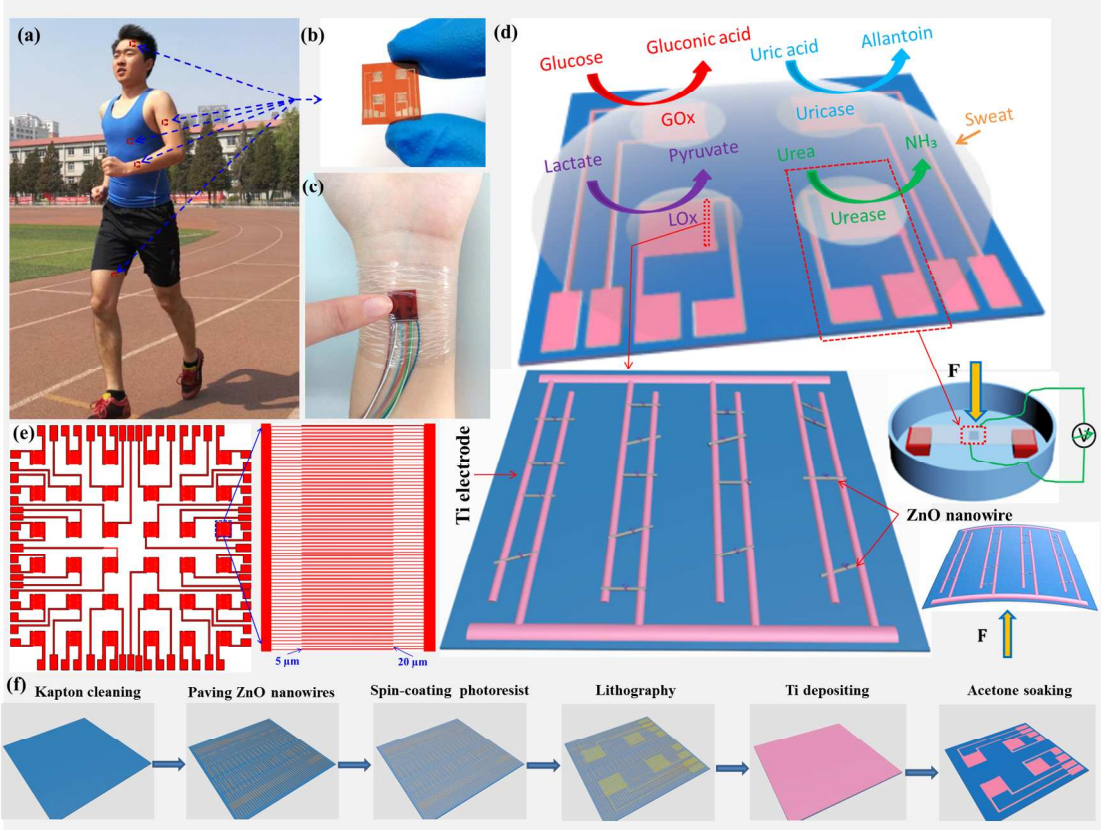

Figure 1. Experimental design, device architecture and fabrication procedure of the self-powered wearable non-invasive electronic-skin. (a) The electronic-skin attached on the surface of a runner at different body parts for monitoring the physiological status by analyzing perspiration components. (b, c) Optical images of the electronic-skin (on human wrist). (d) The experimental design of the electronic-skin for detecting lactate, glucose, uric acid and urea. (e) The whole pattern of the electronic-skin. (f) The fabrication process of the electronic-skin.

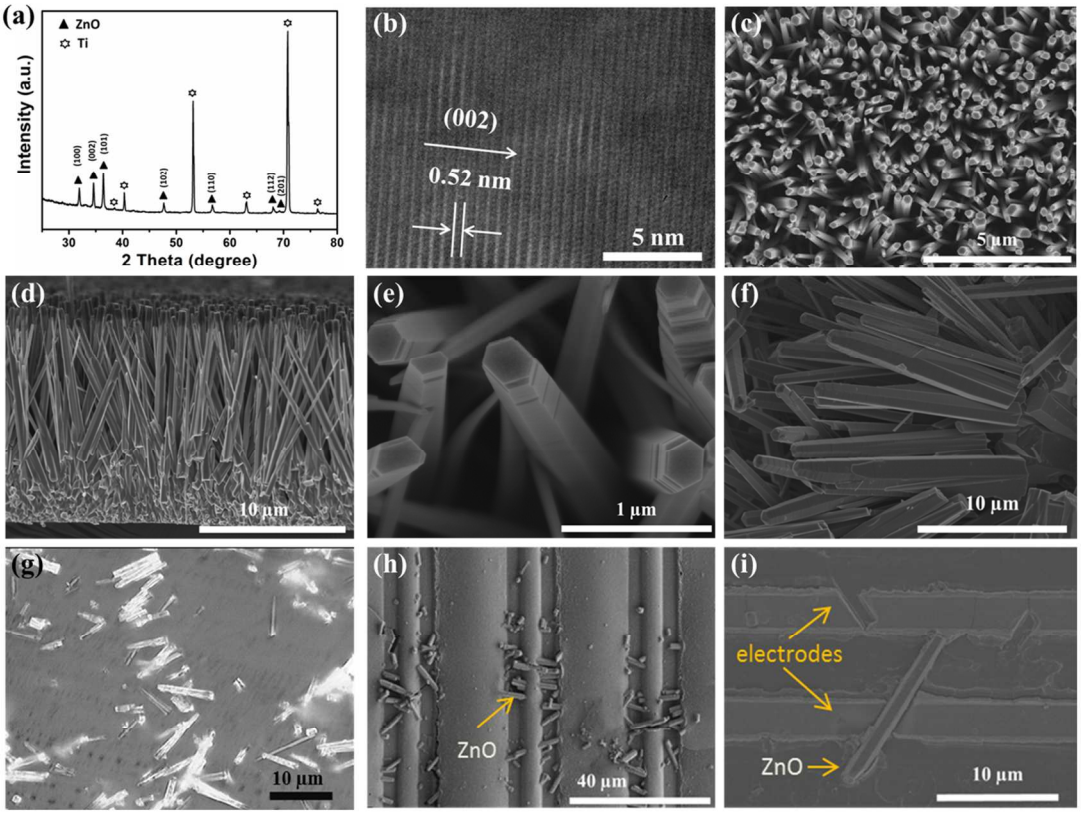

Figure 2. (a) XRD pattern of ZnO nanowire arrays. (b) High-resolution TEM image of ZnO nanowire. (c) The top-view and (d) side-view SEM image of ZnO nanowire arrays. (e) The enlarged view of the heads of ZnO nanowires. (f, g) SEM images of horizontally-aligned ZnO nanowires paving on Ti and Kapton substrate respectively. (h) SEM image of partial region of the electronic-skin (before removing photoresists). (i) SEM image of single ZnO nanowire bridging two Ti electrodes (after removing photoresists).

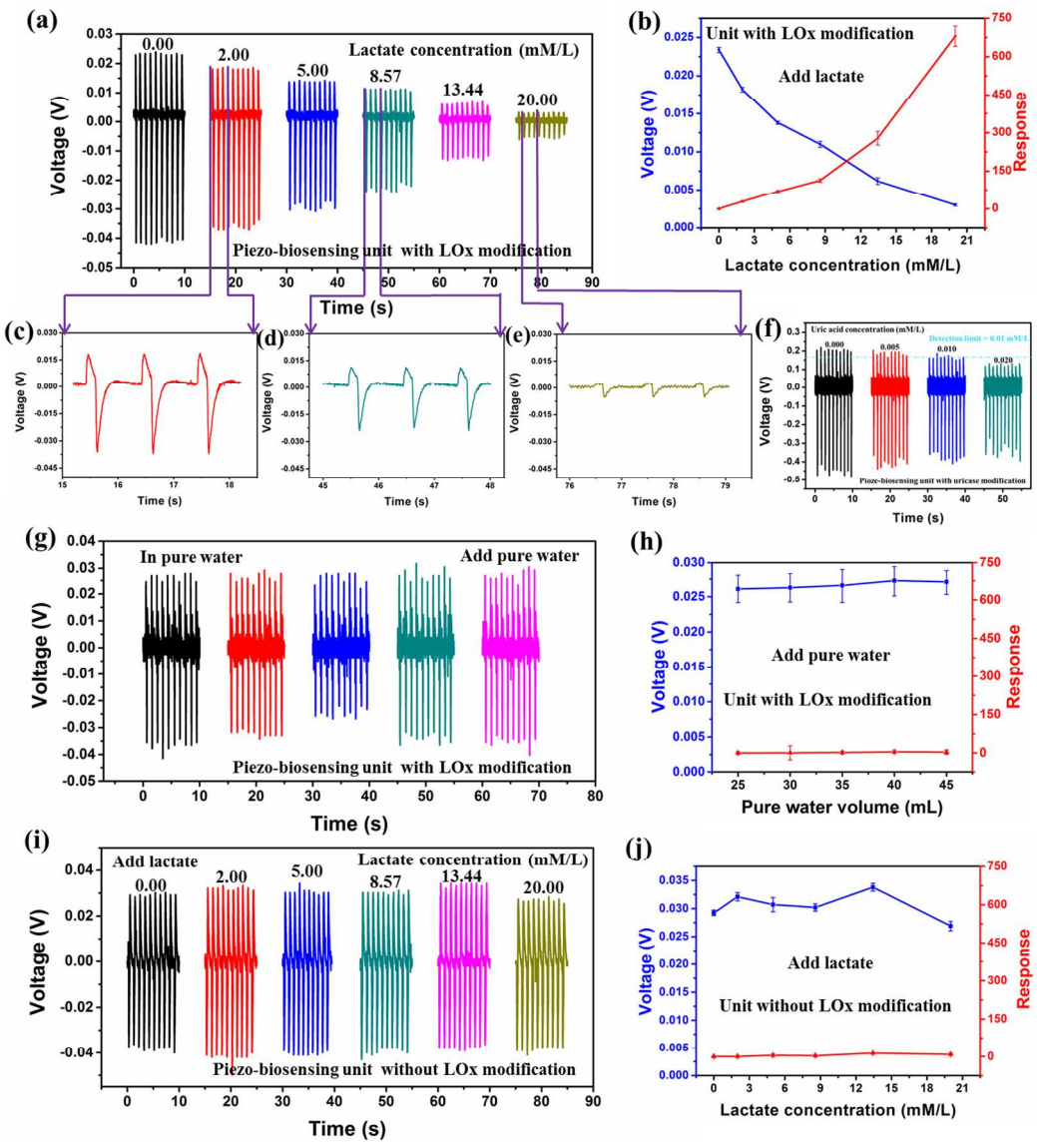

Figure 3. The piezo-lactate-sensing performance of one piezo-biosensing unit (with LOx modification) and the control experiments. (a) The piezoelectric impulse of the piezo-biosensing unit (with LOx modification) under applied deformation with the change of lactate concentration. (b) The outputting piezoelectric voltage and response of the piezo-biosensing unit against different lactate concentrations. (c–e) The piezoelectric output against 2, 8.57 and 20 mM L^{-1} lactate solution. (f) The detection limit and the resolution of the lactate piezo-biosensing unit. (g) The outputting piezoelectric voltage of the piezo-biosensing unit (with LOx modification) in

different volumes of pure water. (h) The outputting piezoelectric voltage and response in pure water. (i) The outputting piezoelectric voltage of the piezo-biosensing unit (without LOx modification) in lactate aqueous solution. (j) The outputting piezoelectric voltage and response of the piezo-biosensing unit (without LOx modification) against different lactate concentrations.

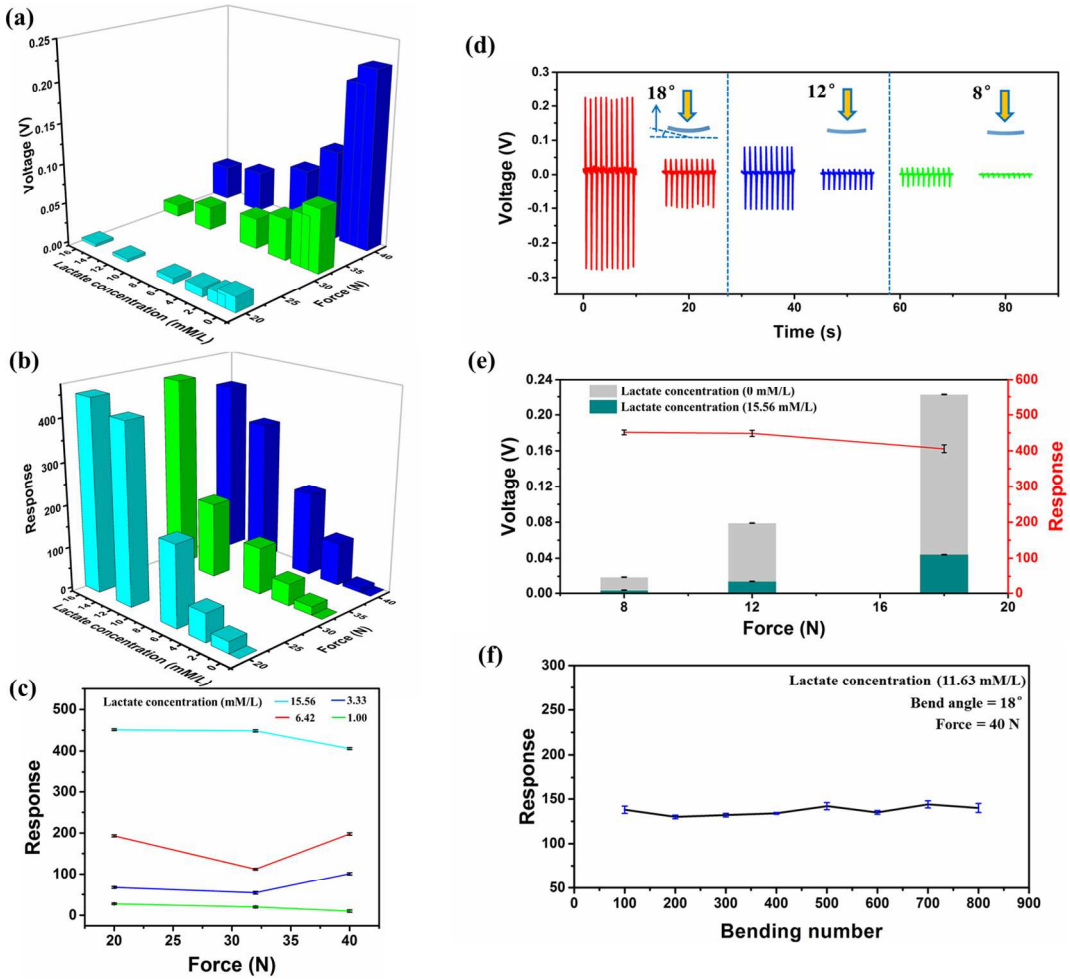

Figure 4. (a) The relationship between the outputting piezoelectric voltage of the piezo-biosensing unit (with LOx modification) in the electronic-skin and lactate concentration under different forces (20, 32, 40 N). (b) The lactate response under different forces. (c) The responses under different forces and lactate concentrations. (d) The outputting piezoelectric voltage of the piezo-biosensing unit (with LOx modification) in the electronic-skin under different bending angles (18°, 12° and 8°). The testing lactate concentration is 15.56 mM L^{-1}. (e) The relationship between piezo-lactate-sensing performance and bending angle. (f) The relationship between response and bending number. The testing lactate concentration is 11.63 mM L^{-1}.

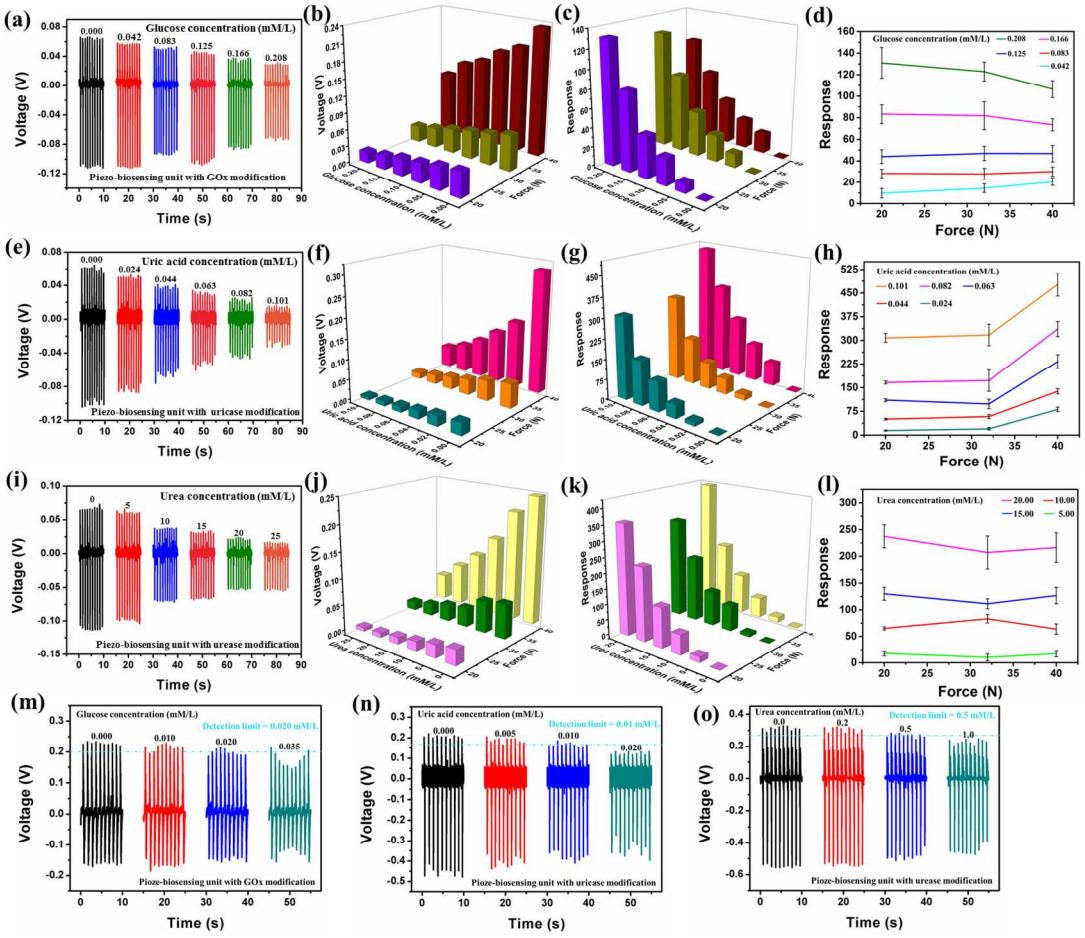

Figure 5. The piezo-sensing performance of the piezo-biosensing units (modified with GOx, uricase and urease) for detecting glucose, uric acid and urea. (a-d) The piezo-glucose-sensing performance of the piezo-biosensing unit modified with GOx under different applied forces. (e-h) The piezo-uric-acid-sensing performance of the piezo-biosensing unit modified with uricase under different applied forces. (i-l) The piezo-urea-sensing performance of the piezo-biosensing unit modified with urease under different applied forces. (m-o) The detection limits of the piezo-biosensing units (modified with GOx, uricase and urease).

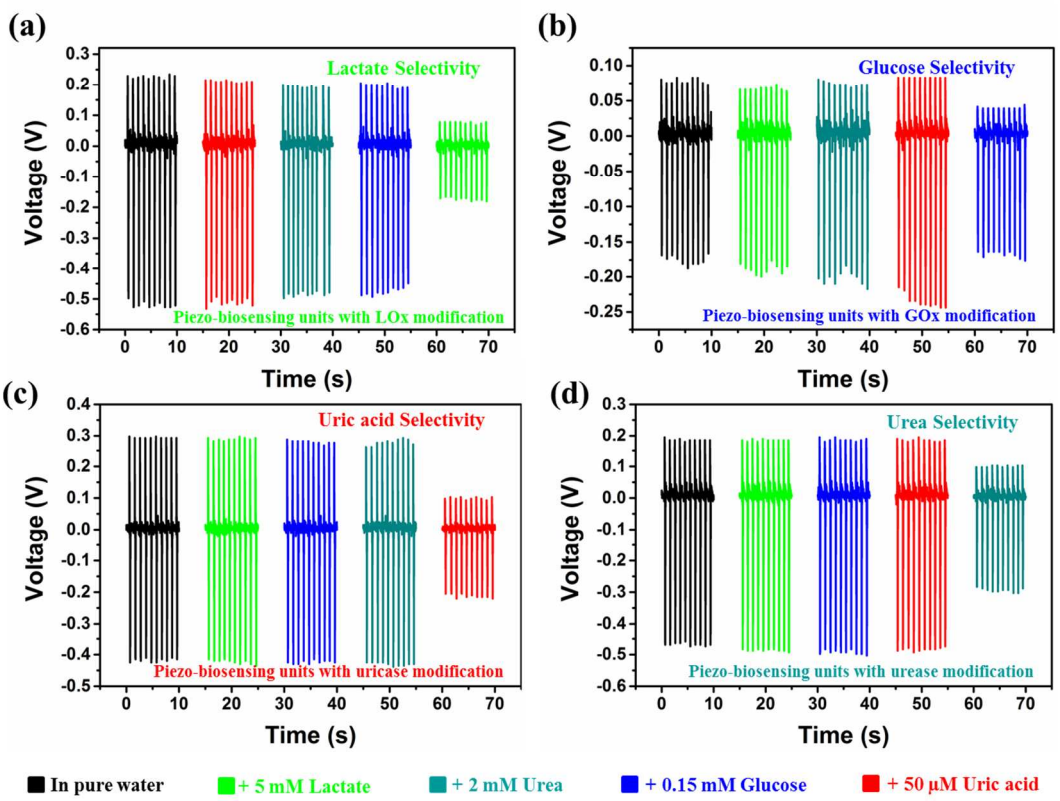

Figure 6. The selectivity of the piezo-biosensing units modified with LOx (a), GOx (b), uricase (c) and urease (d) in the electronic-skin for detecting lactate, glucose, uric acid and urea, respectively.

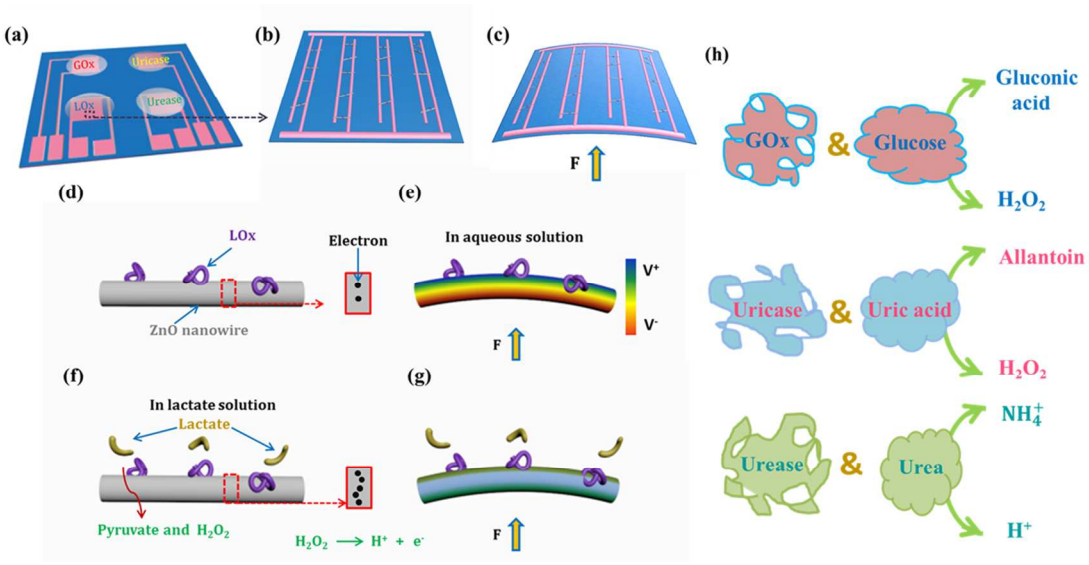

Figure 7. The working mechanism of the self-powered wearable non-invasive electronic-skin for perspiration analysis. (a) The piezo-biosensing units in the electronic-skin are modified with LOx, GOx, uricase and urease, respectively. (b) The enzyme/ZnO nanowires crossing on the interdigital electrodes. (c) The enzyme/ZnO nanowires can be bended under applied force. (d) The LOx/ZnO nanowire in pure water without applied deformation. (e) The piezoelectric potential of LOx/ZnO nanowire in pure water created by applied deformation. (f) The LOx/ZnO nanowire in lactate aqueous solution without applied deformation. (g) The piezoelectric output of LOx/ZnO nanowire in lactate aqueous solution under applied deformation. (h) The enzymatic reactions: GOx and glucose, uricase and uric acid, urease and urea.

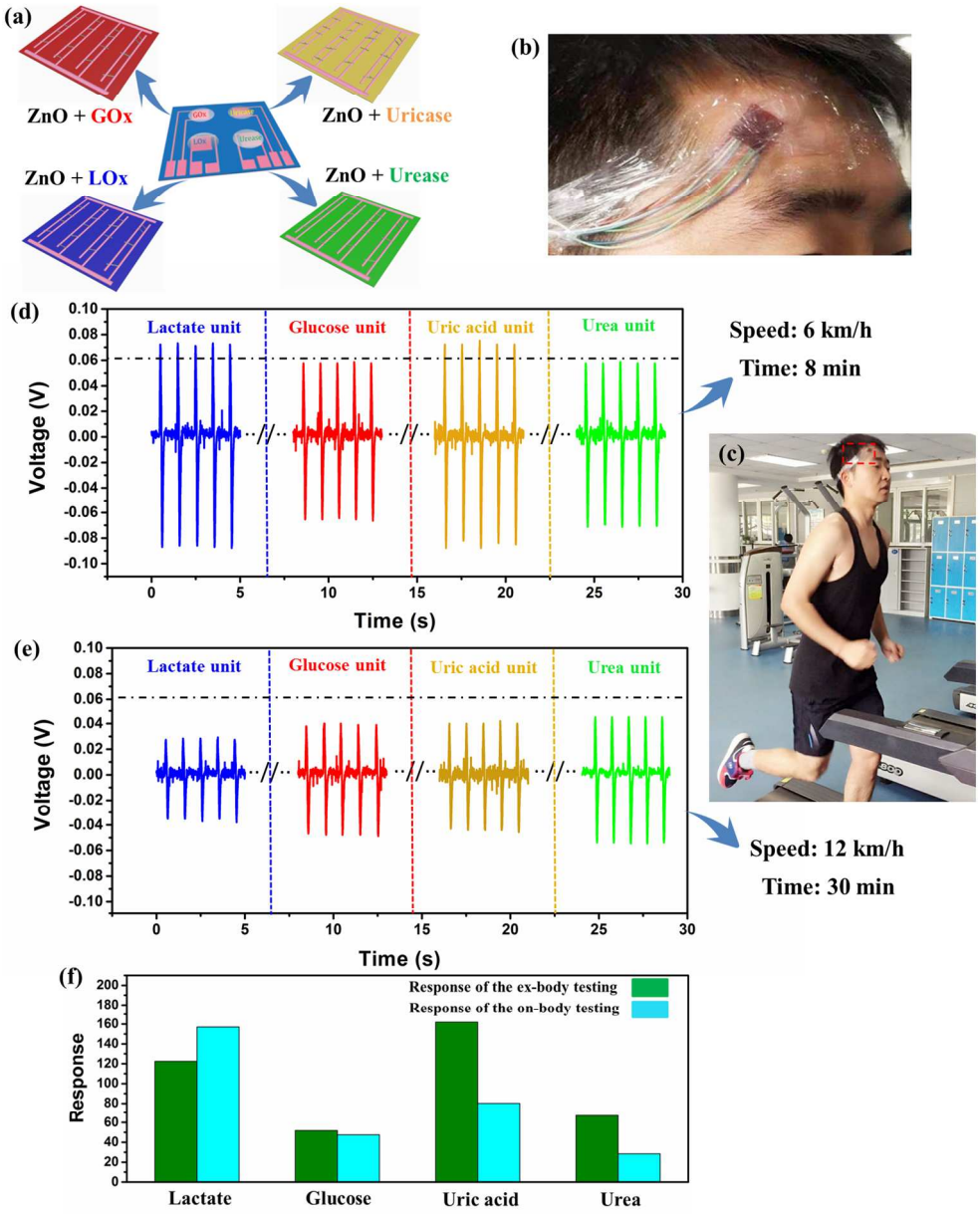

Figure 8. The self-powered wearable non-invasive electronic-skin on the skin of a runner for perspiration analysis (detecting lactate, glucose, uric acid and urea) without any external electricity power supply. (a) The four piezo-biosensing units in the electronic-skin. (b) The electronic-skin is attached on the forehead of a runner. (c) A runner with different speed. (d, e) The piezoelectric output of the four piezo-biosensing units with different running speed and duration. (f) The comparison of the response between on-body and ex-body testing.

REFERENCES

(1) Gibney, E. The Body Electric. *Nature* **2015**, *528*, 26-28.

(2) Austen, K. The Trouble With Wearables. *Nature* **2015**, *525*, 22-24.

(3) Wu, W. Z.; Wang, L.; Li, Y. L.; Zhang, F.; Lin, L.; Niu, S. M.; Chenet, D.; Zhang, X.; Hao, Y. F.; Heinz, T. F.; Hone, J.; Wang, Z. L. Piezoelectricity of Single-Atomic-Layer MoS2 for Energy Conversion and Piezotronics. *Nature* **2014**, *514*, 470-474.

(4) Wang, C.; Hwang, D.; Yu, Z. B.; Takei, K.; Park, J.; Chen, T.; Ma, B. W.; Javey, A. User-Interactive Electronic Skin for Instantaneous Pressure Visualization. *Nat. Mater.* **2013**, *12*, 899-904.

(5) Jian, M. Q.; Xia, K. L.; Wang, Q.; Yin, Z.; Wang, H. M.; Wang, C. Y.; Xie, H. H.; Zhang, M. C.; Zhang, Y. Y. Flexible and Highly Sensitive Pressure Sensors Based on Bionic Hierarchical Structures. *Adv. Funct. Mater.* **2017**, *27*, 1606066.

(6) Xue, X. Y.; Qu, Z.; Fu, Y. M.; Yu, B. W.; Xing, L. L.; Zhang, Y. Self-Powered Electronic-Skin for Detecting Glucose Level in Body Fluid Basing on Piezo-Enzymatic-Reaction Coupling Process. *Nano Energy* **2016**, *26*, 148-156.

(7) Luo, N. Q.; Dai, W. X.; Li, C. L.; Zhou, Z. Q.; Lu, L. Y.; Poon, C. C. Y.; Chen, S. C.; Zhang, Y. T.; Zhao, N. Flexible Piezoresistive Sensor Patch Enabling Ultralow Power Cuffless Blood Pressure Measurement. *Adv. Funct. Mater.* **2016**, *26*, 1178-1187.

(8) Iverson, N. M.; Barone, P. W.; Shandell, M.; Trudel, L. J.; Sen, S.; Sen, F.; Ivanov, V.; Atolia, E.; Farias, E.; McNicholas, T. P.; Reuel, N.; Parry, N. M. A.; Wogan, G. N.; Strano, M. S. In Vivo Biosensing via Tissue-Localizable Near-Infrared-Fluorescent Single-Walled Carbon Nanotubes. *Nat. Nanotechnol.* **2013**, *8*, 873-880.

(9) Khodagholy, D.; Gelinas, J. N.; Thesen, T.; Doyle, W.; Devinsky, O.; Malliaras, G. G.; Buzsaki, G. NeuroGrid: Recording Action Potentials From the Surface of the Brain. *Nat. Neurosci.* **2015**, *18*, 310-315.

(10) Kim, J.; Gutruf, P.; Chiarelli, A. M.; Heo, S. Y.; Cho, K.; Xie, Z. Q.; Banks, A.; Han, S.; Jang, K. I.; Lee, J. W.; Lee, K. T.; Feng, X.; Huang, Y. G.; Fabiani, M.; Gratton, G.; Paik, U.; Rogers, J. A. Miniaturized Battery-Free Wireless Systems for Wearable Pulse Oximetry. *Adv. Funct. Mater.* **2017**, *27*, 1604373.

(11) Ilhan, I.; Yildiz, I.; Kayrak, M. Development of A Wireless Blood Pressure Measuring Device with Smart Mobile Device. *Comput. Meth. Programs Biomed.* **2016**, *125*, 94-102.

(12) Williamson, A.; Rivnay, J.; Kergoat, L.; Jonsson, A.; Inal, S.; Uguz, I.; Ferro, M.; Ivanov, A.; Sjostrom, T. A.; Simon, D. T.; Berggren, M.; Malliaras, G. G.; Bernard, C. Controlling Epileptiform Activity with Organic Electronic Ion Pumps. *Adv. Mater.* **2015**, *27*, 3138-3144.

(13) Bao, R. R.; Wang, C. F.; Dong, L.; Yu, R. M.; Zhao, K.; Wang, Z. L.; Pan, C. F. Flexible and Controllable Piezo-Phototronic Pressure Mapping Sensor Matrix by ZnO NW/p-Polymer LED Array. *Adv. Funct. Mater.* **2015**, *25*, 2884-2891.

(14) Yang, P. K.; Lin, Z. H.; Pradel, K. C.; Lin, L.; Li, X. H.; Wen, X. N.; He, J. H.; Wang, Z. L. Paper-Based Origami Triboelectric Nanogenerators and Self-Powered Pressure Sensors. *ACS Nano* **2015**, *9*, 901-907.

(15) Liang, J. J.; Li, L.; Niu, X. F.; Yu, Z. B.; Pei, Q. B. Elastomeric Polymer Light-Emitting Devices and Displays. *Nat. Photonics* **2013**, *7*, 817-824.

(16) Kim, D. H.; Ghaffari, R.; Lu, N. S.; Rogers, J. A. Flexible and Stretchable Electronics for Biointegrated Devices. In *Annual Review Of Biomedical Engineering, Vol 14*, Yarmush, M. L., Ed. Annual Reviews: Palo Alto, **2012**, pp 113-128.

(17) Patel, S.; Park, H.; Bonato, P.; Chan, L.; Rodgers, M. A Review of Wearable Sensors and Systems with Application in Rehabilitation. *J. NeuroEng. Rehabil.* **2012**, *9*, 21.

(18) Bandodkar, A. J.; Wang, J. Non-Invasive Wearable Electrochemical Sensors: A Review. *Trends Biotechnol.* **2014**, *32*, 363-371.

(19) Wu, N.; Cheng, X. F.; Zhong, Q. Z.; Zhong, J. W.; Li, W. B.; Wang, B.; Hu, B.; Zhou, J. Cellular Polypropylene Piezoelectret for Human Body Energy Harvesting and Health Monitoring. *Adv. Funct. Mater.* **2015**, *25*, 4788-4794.

(20) Schazmann, B.; Morris, D.; Slater, C.; Beirne, S.; Fay, C.; Reuveny, R.; Moyna, N.; Diamond, D. A Wearable Electrochemical Sensor for the Real-Time Measurement of Sweat Sodium Concentration. *Anal. Methods* **2010**, *2*, 342-348.

(21) Jia, W. Z.; Bandodkar, A. J.; Valdes-Ramirez, G.; Windmiller, J. R.; Yang, Z. J.; Ramirez, J.; Chan, G.; Wang, J. Electrochemical Tattoo Biosensors for Real-Time Noninvasive Lactate Monitoring in Human Perspiration. *Anal. Chem.* **2013**, *85*, 6553-6560.

(22) Bandodkar, A. J.; Molinnus, D.; Mirza, O.; Guinovart, T.; Windmiller, J. R.; Valdes-Ramirez, G.; Andrade, F. J.; Schoning, M. J.; Wang, J. Epidermal Tattoo Potentiometric Sodium Sensors with Wireless Signal Transduction for Continuous Non-Invasive Sweat Monitoring. *Biosens. Bioelectron.* **2014**, *54*, 603-609.

(23) Rose, D. P.; Ratterman, M. E.; Griffin, D. K.; Hou, L. L.; Kelley-Loughnane, N.; Naik, R. R.; Hagen, J. A.; Papautsky, I.; Heikenfeld, J. C. Adhesive RFID Sensor Patch for Monitoring of Sweat Electrolytes. *IEEE Trans. Biomed. Eng.* **2015**, *62*, 1457-1465.

(24) Emaminejad, S.; Gao, W.; Wu, E.; Davies, Z. A.; Nyein, H. Y. Y.; Challa, S.; Ryan, S. P.; Fahad, H. M.; Chen, K.; Shahpar, Z.; Talebi, S.; Milla, C.; Javey, A.; Davis, R. W. Autonomous

Sweat Extraction and Analysis Applied to Cystic Fibrosis and Glucose Monitoring Using a Fully Integrated Wearable Platform. *Proc. Natl. Acad. Sci. U.S.A.* **2017**, *114*, 4625-4630.

(25) Gao, W.; Emaminejad, S.; Nyein, H. Y. Y.; Challa, S.; Chen, K. V.; Peck, A.; Fahad, H. M.; Ota, H.; Shiraki, H.; Kiriya, D.; Lien, D. H.; Brooks, G. A.; Davis, R. W.; Javey, A. Fully Integrated Wearable Sensor Arrays for Multiplexed in Situ Perspiration Analysis. *Nature* **2016**, *529*, 509-514.

(26) Ma, Y. J.; Jang, K. I.; Wang, L.; Jung, H. N.; Kwak, J. W.; Xue, Y. G.; Chen, H.; Yang, Y. Y.; Shi, D. W.; Feng, X.; Rogers, J. A.; Huang, Y. G. Design of Strain-Limiting Substrate Materials for Stretchable and Flexible Electronics. *Adv. Funct. Mater.* **2016**, *26*, 5345-5351.

(27) Wang, Y.; Wang, L.; Yang, T. T.; Li, X.; Zang, X. B.; Zhu, M.; Wang, K. L.; Wu, D. H.; Zhu, H. W. Wearable and Highly Sensitive Graphene Strain Sensors for Human Motion Monitoring. *Adv. Funct. Mater.* **2014**, *24*, 4666-4670.

(28) Imani, S.; Bandodkar, A. J.; Mohan, A. M. V.; Kumar, R.; Yu, S. F.; Wang, J.; Mercier, P. P. A Wearable Chemical-Electrophysiological Hybrid Biosensing System for Real-Time Health and Fitness Monitoring. *Nat. Commun.* **2016**, *7*, 11650.

(29) Lee, J. W.; Xu, R. X.; Lee, S.; Jang, K. I.; Yang, Y. C.; Banks, A.; Yu, K. J.; Kim, J.; Xu, S.; Ma, S. Y.; Jang, S. W.; Won, P.; Li, Y. H.; Kim, B. H.; Choe, J. Y.; Huh, S.; Kwon, Y. H.; Huang, Y. G.; Paik, U.; Rogers, J. A. Soft, Thin Skin-Mounted Power Management Systems and Their Use in Wireless Thermography. *Proc. Natl. Acad. Sci. U. S. A.* **2016**, *113*, 6131-6136.

(30) Wang, X. F.; Lu, X. H.; Liu, B.; Chen, D.; Tong, Y. X.; Shen, G. Z. Flexible Energy-Storage Devices: Design Consideration and Recent Progress. *Adv. Mater.* **2014**, *26*, 4763-4782.

(31) Chong, W. G.; Huang, J. Q.; Xu, Z. L.; Qin, X. Y.; Wang, X. Y.; Kim, J. K. Lithium-Sulfur Battery Cable Made from Ultralight, Flexible Graphene/Carbon Nanotube/Sulfur Composite Fibers. *Adv. Funct. Mater.* **2017**, *27*, 1604815.

(32) Huang, Y.; Zhu, M. S.; Huang, Y.; Pei, Z. X.; Li, H. F.; Wang, Z. F.; Xue, Q.; Zhi, C. Y. Multifunctional Energy Storage and Conversion Devices. *Adv. Mater.* **2016**, *28*, 8344-8364.

(33) Sonner, Z.; Wilder, E.; Heikenfeld, J.; Kasting, G.; Beyette, F.; Swaile, D.; Sherman, F.; Joyce, J.; Hagen, J.; Kelley-Loughnane, N.; Naik, R. The Microfluidics of The Eccrine Sweat Gland, Including Biomarker Partitioning, Transport, and Biosensing Implications. *Biomicrofluidics* **2015**, *9*, 031301.

(34) Minami, T.; Sato, T.; Minamiki, T.; Fukuda, K.; Kumaki, D.; Tokito, S. A Novel OFET-Based Biosensor for the Selective and Sensitive Detection of Lactate Levels. *Biosens. Bioelectron.* **2015**, *74*, 45-48.

(35) Labroo, P.; Cui, Y. Flexible Graphene Bio-Nanosensor for Lactate. *Biosens. Bioelectron.* **2013**, *41*, 852-856.

(36) Lamas-Ardisana, P. J.; Loaiza, O. A.; Anorga, L.; Jubete, E.; Borghei, M.; Ruiz, V.; Ochoteco, E.; Cabanero, G.; Grande, H. J. Disposable Amperometric Biosensor Based on Lactate Oxidase Immobilised on Platinum Nanoparticle-Decorated Carbon Nanofiber and Poly(Diallyldimethylammonium Chloride) Films. *Biosens. Bioelectron.* **2014**, *56*, 345-351.

(37) Derbyshire, P. J.; Barr, H.; Davis, F.; Higson, S. P. J. Lactate in Human Sweat: A Critical Review of Research to the Present Day. *J. Physiol. Sci.* **2012**, *62*, 429-440.

(38) Ma, S. W.; Zhang, X. H.; Liao, Q. L.; Liu, H. S.; Huang, Y. H.; Song, Y.; Zhao, Y. G.; Zhang, Y. Enzymatic Lactic Acid Sensing by In-Doped ZnO Nanowires Functionalized AlGaAs/GaAs High Electron Mobility Transistor. *Sens. Actuator B-Chem.* **2015**, *212*, 41-46.

(39) Talary, M. S.; Dewarrat, F.; Huber, D.; Caduff, A. In Vivo Life Sign Application of Dielectric Spectroscopy and Non-Invasive Glucose Monitoring. *J. Non-Cryst. Solids* **2007**, *353*, 4515-4517.

(40) Fang, A. J.; Wu, Q. Q.; Lu, Q. J.; Chen, H. Y.; Li, H. T.; Liu, M. L.; Zhang, Y. Y.; Yao, S. Z. Upconversion Ratiometric Fluorescence and Colorimetric Dual-Readout Assay for Uric Acid. *Biosens. Bioelectron.* **2016**, *86*, 664-670.

(41) Sugase, S.; Tsuda, T. Determination of Lactic Acid, Uric Acid, Xanthine and Tyrosine in Human Sweat by HPLC, and The Concentration Variation of Lactic Acid in It After The Intake of Wine. *Bunseki Kagaku* **2002**, *51*, 429-435.

(42) Melzer, K.; Bhatt, V. D.; Jaworska, E.; Mittermeier, R.; Maksymiuk, K.; Michalska, A.; Lugli, P. Enzyme Assays Using Sensor Arrays Based on Ion-Selective Carbon Nanotube Field-Effect Transistors. *Biosens. Bioelectron.* **2016**, *84*, 7-14.

(43) Corrie, S. R.; Coffey, J. W.; Islam, J.; Markey, K. A.; Kendall, M. A. F. Blood, Sweat, and Tears: Dveloping Clinically Relevant Protein Biosensors for Integrated Body Fluid Analysis. *Analyst* **2015**, *140*, 4350-4364.

(44) Ma, S. S.; Xue, J. J.; Zhou, Y. M.; Zhang, Z. W. Photochemical Synthesis of ZnO/Ag2O Heterostructures with Enhanced Ultraviolet and Visible Photocatalytic Activity. *J. Mater. Chem. A* **2014**, *2*, 7272-7280.

(45) Zhang, L. L.; Fu, Y. M.; Xing, L. L.; Liu, B. D.; Zhang, Y.; Xue, X. Y. A Self-Powered Flexible Vision Electronic-Skin for Image Recognition Based on a Pixel-Addressable Matrix of Piezophototronic ZnO Nanowire Arrays. *J. Mater. Chem. C* **2017**, *5*, 6005-6013.

(46) Zhang, L.; Bai, S.; Su, C.; Zheng, Y. B.; Qin, Y.; Xu, C.; Wang, Z. L. A High-Reliability Kevlar Fiber-ZnO Nanowires Hybrid Nanogenerator and Its Application on Self-Powered UV Detection. *Adv. Funct. Mater.* **2015**, *25*, 5794-5798.

(47) Kevin, M.; Fou, Y. H.; Wong, A. S. W.; Ho, G. W. A Novel Maskless Approach Towards Aligned, Density Modulated and Multi-Junction ZnO Nanowires for Enhanced Surface Area and Light Trapping Solar Cells. *Nanotechnology.* **2010**, *21* (31), 315602.

(48) Kevin, M.; Lee, G. H.; Ho, G. W. Non-Planar Geometries of Solution Processable Transparent Conducting Oxide: From Film Characterization to Architectured Electrodes. *Energy Environ. Sci.* **2012**, *5* (5), 7196-7202.

(49) Ju, S. Y.; Facchetti, A.; Xuan, Y.; Liu, J.; Ishikawa, F.; Ye, P. D.; Zhou, C. W.; Marks, T. J.; Janes, D. B. Fabrication of Fully Transparent Nanowire Transistors for Transparent and Flexible Electronics. *Nat. Nanotechnol.* **2007**, *2*, 378-384.

(50) Su, Y. J.; Wen, X. N.; Zhu, G.; Yang, J.; Chen, J.; Bai, P.; Wu, Z. M.; Jiang, Y. D.; Wang, Z. L. Hybrid Triboelectric Nanogenerator for Harvesting Water Wave Energy and as a Self-Powered Distress Signal Emitter. *Nano Energy.* **2014**, *9*, 186-195.

(51) Choi, M. Y.; Choi, D.; Jin, M. J.; Kim, I.; Kim, S. H.; Choi, J. Y.; Lee, S. Y.; Kim, J. M.; Kim, S. W. Mechanically Powered Transparent Flexible Charge-Generating Nanodevices with Piezoelectric ZnO Nanorods. *Adv. Mater.* **2009**, *21*, 2185-2189.

(52) Guo, L.; Ji, Y. L.; Xu, H. B.; Simon, P.; Wu, Z. Y. Regularly Shaped, Single-Crystalline ZnO Nanorods with Wurtzite Structure. *J. Am. Chem. Soc.* **2002**, *124*, 14864-14865.

(53) Lao, J. Y.; Huang, J. Y.; Wang, D. Z.; Ren, Z. F. ZnO Nanobridges and Nanonails. *Nano Lett.* **2003**, *3*, 235-238.

(54) Zang, W. L.; Nie, Y. X.; Zhu, D.; Deng, P.; Xing, L. L.; Xue, X. Y. Core-Shell In2O3/ZnO Nanoarray Nanogenerator as a Self-Powered Active Gas Sensor with High H2S Sensitivity and Selectivity at Room Temperature. *J. Phys. Chem. C* **2014**, *118*, 9209-9216.

(55) Bartlett, M. D.; Markvicka, E. J.; Majidi, C. Rapid Fabrication of Soft, Multilayered Electronics for Wearable Biomonitoring. *Adv. Funct. Mater.* **2016**, *26*, 8496-8504.

(56) Guan, L. Y.; Nilghaz, A.; Su, B.; Jiang, L.; Cheng, W. L.; Shen, W. Stretchable-Fiber-Confined Wetting Conductive Liquids as Wearable Human Health Monitors. *Adv. Funct. Mater.* **2016**, *26*, 4511-4517.

(57) Kong, X. Y.; Wang, Z. L. Spontaneous Polarization-Induced Nanohelixes, Nanosprings, and Nanorings of Piezoelectric Nanobelts. *Nano Lett.* **2003**, *3*, 1625-1631.

(58) Wang, Z. L.; Kong, X. Y.; Ding, Y.; Gao, P. X.; Hughes, W. L.; Yang, R. S.; Zhang, Y. Semiconducting and Piezoelectric Oxide Nanostructures Induced by Polar Surfaces. *Adv. Funct. Mater.* **2004**, *14*, 943-956.

(59) Qu, Z.; Fu, Y. M.; Yu, B. W.; Deng, P.; Xing, L. L.; Xue, X. Y. High and Fast H2S Response of NiO/ZnO Nanowire Nanogenerator as a Self-Powered Gas Sensor. *Sens. Actuator B-Chem.* **2016**, *222*, 78-86.

(60) Zhang, H. L.; Yang, Y.; Hou, T. C.; Su, Y. J.; Hu, C. G.; Wang, Z. L. Triboelectric Nanogenerator Built Inside Clothes for Self-Powered Glucose Biosensors. *Nano Energy* **2013**, *2*, 1019-1024.

(61) Zhao, Y. Y.; Lai, X.; Deng, P.; Nie, Y. X.; Zhang, Y.; Xing, L. L.; Xue, X. Y. Pt/ZnO Nanoarray Nanogenerator as Self-Powered Active Gas Sensor with Linear Ethanol Sensing at Room Temperature. *Nanotechnology* **2014**, *25*, 115502.

(62) Lin, Y. J.; Deng, P.; Nie, Y. X.; Hu, Y. F.; Xing, L. L.; Zhang, Y.; Xue, X. Y. Room-Temperature Self-Powered Ethanol Sensing of a Pd/ZnO Nanoarray Nanogenerator Driven by Human Hinger Movement. *Nanoscale* **2014**, *6*, 4604-4610.

(63) Nie, Y. X.; Deng, P.; Zhao, Y. Y.; Wang, P. L.; Xing, L. L.; Zhang, Y.; Xue, X. Y. The Conversion of PN-Junction Influencing the Piezoelectric Output of a CuO/ZnO Nanoarray Nanogenerator and Its Application as a Room-Temperature Self-Powered Active H2S Sensor. *Nanotechnology* **2014**, *25*, 265501.

(64) Weber, J.; Kumar, A.; Kumar, A.; Bhansali, S. Novel Lactate and pH Biosensor for Skin and Sweat Analysis Based on Single Walled Carbon Nanotubes. *Sens. Actuators B* **2006**, *117*, 308-313.

(65) Ahmad, M.; Pan, C. F.; Luo, Z. X.; Zhu, J. A Single ZnO Nanofiber-Based Highly Sensitive Amperometric Glucose Biosensor. *J. Phys. Chem. C* **2010**, *114*, 9308-9313.

(66) Yu, R. M.; Pan, C. F.; Chen, J.; Zhu, G.; Wang, Z. L. Enhanced Performance of a ZnO Nanowire-Based Self-Powered Glucose Sensor by Piezotronic Effect. *Adv. Funct. Mater.* **2013**, *23*, 5868-5874.

(67) Lei, Y. J.; Sun, R. Z.; Zhang, X. C.; Feng, X. J.; Jiang, L. Oxygen-Rich Enzyme Biosensor Based on Superhydrophobic Electrode. *Adv. Mater.* **2016**, *28*, 1477-1481.

(68) Long, Q.; Fang, A. J.; Wen, Y. Q.; Li, H. T.; Zhang, Y. Y.; Yao, S. Z. Rapid and Highly-Sensitive Uric Acid Sensing Based on Enzymatic Catalysis-Induced Upconversion Inner Filter Effect. *Biosens. Bioelectron.* **2016**, *86*, 109-114.

(69) Liu, X. X.; Yang, J. Q.; Sun, S. C.; Guo, L. P.; Yang, L. Enzyme and Inhibition Assay of Urease by Continuous Monitoring of the Ammonium Formation Based on Capillary Electrophoresis. *Electrophoresis* **2016**, *37*, 2692-2698.

(70) Buono, M. J.; Lee, N. V. L.; Miller, P. W. The Relationship Between Exercise Intensity and the Sweat Lactate Excretion Rate. *J. Physiol. Sci.* **2010,** *60* (2), 103-107.

(71) Anastasova, S.; Crewther, B.; Bembnowicz, P.; Curto, V.; Ip, H. M.; Rosa, B.; Yang, G. Z. A Wearable Multisensing Patch for Continuous Sweat Monitoring. *Biosens. Bioelectron.* **2017,** *94*, 730-730.

(72) Dutkiewicz, E. P.; Lin, J. D.; Tseng, T. W.; Wang, Y. S.; Urban, P. L. Hydrogel Micropatches for Sampling and Profiling Skin Metabolites. *Anal. Chem.* **2014,** *86* (5), 2337-2344.

(73) Al-omari, M.; Liu, G. C.; Mueller, A.; Mock, A.; Ghosh, R. N.; Smith, K.; Kaya, T. A Portable Optical Human Sweat Sensor. *J. Appl. Phys.* **2014,** *116* (18), 183102.

Table of Contents